

High dimensional discriminant rules with shrinkage estimators of covariance matrix and mean vector

Jaehoan Kim,^{*} Hoyoung Park,[†] and Junyong Park[‡]

November 2022

Abstract

Linear discriminant analysis is a typical method used in the case of large dimension and small samples. There are various types of linear discriminant analysis methods, which are based on the estimations of the covariance matrix and mean vectors. Although there are many methods for estimating the inverse matrix of covariance and the mean vectors, we consider shrinkage methods based on non-parametric approach. In the case of the precision matrix, the methods based on either the sparsity structure or the data splitting are considered. Regarding the estimation of mean vectors, nonparametric empirical Bayes (NPEB) estimator and nonparametric maximum likelihood estimation (NPMLE) methods are adopted which are also called f -modeling and g -modeling, respectively. We analyzed the performances of linear discriminant rules which are based on combined estimation strategies of the covariance matrix and mean vectors. In particular, we present a theoretical result on the performance of the NPEB method and compare that with the results from other methods in previous studies. We provide simulation studies for various structures of covariance matrices and mean vectors to evaluate the methods considered in this paper. In addition, real data examples such as gene expressions and EEG data are presented.

^{*}Department of Statistics, Texas A&M University, TX, USA, k1mjh6561@tamu.edu

[†]Department of Statistics, Sookmyung Women's University, Seoul, Korea, hyparks@sookmyung.ac.kr

[‡]Department of Statistics, Seoul National University, Seoul, Korea, junyongpark@snu.ac.kr

Keywords : High dimensional discriminant analysis; Nonparametric maximum likelihood estimation; Nonparametric empirical Bayes; Estimation of precision matrix

1 Introduction

In this paper, we consider linear discriminant rule that play an important role in high-dimensional discriminant analysis. Traditionally, Fisher's linear discriminant rule is the most widely used, and it consists of a formula of a mean vector and a covariance matrix. In the case of high dimensionality, the problem of the estimation of the covariance matrix has been treated seriously, for example diagonal matrix or some regularized estimators of covariance matrix. On the other hand, the estimation of the mean vector has been substituted by sample mean vectors, which has received relatively little attention compared to the estimation of the covariance matrix. The covariance matrix and the mean vectors can be estimated under appropriate conditions in high dimension, however, to the best of our knowledge, the performance of the Fisher's rule with those estimates is not well understood such that why and when specific estimates of covariance matrix and mean vectors produce a good performance.

There have been many studies on overcoming the difficulty in high dimensional classification. One most basic approach is a naive Bayes rule which is based on independence assumption. Since the naive Bayes rule utilizes all variables, it may not be efficient under some specific structure such as sparsity situation of mean vector in that only a small proportion of components in mean vector is non zero. On the other hand, the FAIR (feature annealed independent rule) in [4] uses the idea of truncation of coefficients in naive Bayes rule to be efficient in sparse case. To remedy the sensitivity of the naive Bayes rule and the FAIR for various structure of mean vector, lots of attempts have been made to compensate for these shortcomings. For example, [6] approximated the coefficients of the linear discriminant rule using the nonparametric empirical Bayes (NPEB) method by using the f -modeling method mentioned in [3] to minimize the square error of the Bayes rule. This method can be seen as improving the method of the naive Bayes rule by showing good performance even in

relatively sparse cases. In addition, [2] improve the performance of the naive Bayes rule by using so-called g -modeling in [3], which approximates the Bayes estimator of the mean vector using the method of directly estimating the prior distribution of mean values. These methods using f -modeling and g -modeling are based on independence assumption which ignores correlations among all variables although there may exist correlations among variables.

Instead of independent assumption, there has been another approach which consider regularized covariance estimator in Fisher's rule. In general, it is difficult to estimate general covariance matrix in high dimension, however under some restriction such as sparsity or moderately high dimensional case, one can estimate the covariance matrix or precision matrix, for example estimation of sparseness covariance matrix or through re-sampling methods in [5] and [8], respectively. Using the estimated precision matrix, we can decorrelate the observed vectors to decorrelate the data so that we have approximately independent variables and apply discriminant rules based on independent assumption to decorrelated data.

In this paper, we investigate the effect of such decorrelations based on estimate of precision matrix. In particular, we focus on how the performance changes of various methods occur according to the structural change of the mean vector, and we will examine how this affects the structure of the covariance matrix and estimation methods accordingly.

This paper is organized as follows. In section 2, we review the Fisher's rule and estimation of covariance matrix and mean vector. In section 3, we provide the asymptotic results for nonparametric empirical Bayes method and comparison with other methods. Section 4 includes simulations studies to evaluate all the discriminant rules considered in this paper for various combinations of mean vectors and covariance matrices. In section 5, real data examples are also presented to compare all the discriminant rules. We summarize all the results in section 6 as concluding remarks.

2 Estimation of precision matrix and mean vector

In this section, we review the methods of estimating precision matrix and mean vector in high dimension. Throughout this paper, we assume $\mathbf{X}_{ij} \sim N_p(\boldsymbol{\mu}_i, \Sigma)$ for $i = 0, 1$ and $j = 1, \dots, n_i$.

A well known linear discriminant rule, Fisher’s linear discriminant analysis (LDA), is

$$\delta(\mathbf{x}^{new}) = \frac{1}{2}[1 - \text{sign}\{f(\mathbf{x}^{new})\}]$$

where

$$f(\mathbf{x}^{new}) = \left(\mathbf{x}^{new} - \frac{\boldsymbol{\mu}_1 + \boldsymbol{\mu}_2}{2}\right)^\top \boldsymbol{\Sigma}^{-1}(\boldsymbol{\mu}_1 - \boldsymbol{\mu}_2). \quad (1)$$

As one can see, Fisher’s LDA requests two estimates, $\boldsymbol{\mu}_i$ and $\Omega = \boldsymbol{\Sigma}^{-1}$.

First, when estimating $\boldsymbol{\Sigma}$, difficulty arises in high dimensional situations since the sample covariance matrix is not invertible. Therefore, there exist several alternatives to estimate Ω directly in high dimensional situation. In this paper, we utilized the precision estimation methods using 1) L^1 penalty of precision matrix (which is called graphical Lasso method; we call this method ‘glasso’ in this paper; see [5]) and 2) random sample splitting (we call this method ‘LAM’; see [8]). Of course, we can assume the precision matrix to be diagonal and naively estimate each element. We write this method as ‘IR’, which is the shorthand of ‘Independence Rule’.

Regarding the estimation of $\boldsymbol{\mu}_i$, we use two methods based on two types of nonparametric empirical Bayes estimations, namely g -modeling and f -modeling introduced in [3]. Such mean vector estimations have been used in [6] and [2] under independent assumption of variables. Obviously, we also consider the sample mean as an estimate of $\boldsymbol{\mu}_i$.

The mainstream of this paper is to examine the performance of different types of discriminant rules in high dimensional situations and analyze its performance both practically and theoretically.

As a building block, we define the decorrelated data matrix \mathbf{Z} as

$$\mathbf{Z}_{ij} = \Omega^{1/2}\mathbf{X}_{ij} \sim N(\Omega^{1/2}\boldsymbol{\mu}_i, I_p) \equiv N_p(\boldsymbol{\mu}_i^*, I_p) \quad (2)$$

where I_p is $p \times p$ identity matrix. Based on \mathbf{Z}_{ij} , the Fisher’s rule is expressed as follows:

$$\begin{aligned}
f(\mathbf{x}^{new}) &= \left(\mathbf{x}^{new} - \frac{\boldsymbol{\mu}_1 + \boldsymbol{\mu}_2}{2} \right)^\top \boldsymbol{\Sigma}^{-1} (\boldsymbol{\mu}_1 - \boldsymbol{\mu}_2) \\
&= \{ \boldsymbol{\Sigma}^{-1/2} (\boldsymbol{\mu}_1 - \boldsymbol{\mu}_2) \}^\top \boldsymbol{\Sigma}^{-1/2} \left(\mathbf{x}^{new} - \frac{\boldsymbol{\mu}_1 + \boldsymbol{\mu}_2}{2} \right)^\top \\
&= (\boldsymbol{\mu}_1^* - \boldsymbol{\mu}_2^*)^\top \left(\mathbf{z}^{new} - \frac{\boldsymbol{\mu}_1^* + \boldsymbol{\mu}_2^*}{2} \right) \\
&\equiv \sum_{i=1}^p a_i z_i^{new} + a_0
\end{aligned} \tag{3}$$

where $\mathbf{z}^{new} = \boldsymbol{\Sigma}^{-1/2} \mathbf{x}^{new}$, $a_i = \mu_{1i}^* - \mu_{2i}^*$ and $a_0 = -(\boldsymbol{\mu}_1^* - \boldsymbol{\mu}_2^*)^\top (\boldsymbol{\mu}_1^* + \boldsymbol{\mu}_2^*) / 2$.

In practice, $\boldsymbol{\Omega} = \boldsymbol{\Sigma}^{-1}$ is unknown, so we need to estimate $\hat{\boldsymbol{\Omega}}$ and decorrelate X with $\hat{\boldsymbol{\Omega}}^{1/2}$. If such estimates are accurate, it is expected that all transformed variables \mathbf{Z}_{ij} are almost independent and then we can apply discriminant rules derived from independent assumption to decorrelated data in (2).

To summarize, we have two components in estimating Fisher's discriminant rule : one is for estimating $\boldsymbol{\Omega}$ or $\boldsymbol{\Sigma}$ and the other for estimating $\boldsymbol{\mu}_i^*$ based on \mathbf{Z}_{ij} . We present these two procedures in the following sections.

2.1 Estimation of precision matrix

In the case of the precision matrix, there are two directions : one is based on estimation under some special structural assumptions and the other one is for general case without any structural assumption. In the former case, it is mainly assumed that precision matrix has sparsity or graphical structure such as [5], however, this structural assumption has limitation for general multivariate data. On the other hand, the latter case is for estimating precision matrix without structural assumption as in [8], however the dimension has limitation compared to the former case.

We denote the covariance matrix and precision matrix as $\boldsymbol{\Sigma}$ and $\boldsymbol{\Omega}$, respectively. Throughout this paper, we consider two methods : the method based on graphical model, called glasso

in [5] and the other method based on random sample splitting of data, called LAM method in [8].

First, the algorithm of glasso is initially devised to estimate precision matrix under sparsity assumption. To utilize this assumption, the problem of maximizing a penalized log-likelihood function with respect to the matrix Θ arises. Penalty term is L_1 -norm of the precision matrix. The objective function in glasso is written as

$$f(\Theta) = \log \det(\Theta) - \text{tr}(S_n \Theta) - \rho \|\Theta\|_1 \quad (4)$$

where S_n is sample covariance matrix, $\det(\Theta)$ is the determinant of Θ and ρ is the regularization parameter. The optimal value of Θ maximizing the function above is used as the estimator of Ω .

Secondly, LAM algorithm uses random sample splitting idea. Since S_n is full rank for $n > p$, S_n^{-1} can be used as the estimator of precision matrix. For high dimensional data, however, since S_n is not invertible, this method is not applicable anymore. To avoid this problem, [8] applied following strategy to make the estimator of covariance matrix invertible. Σ can be represented as

$$\Sigma = PDP^T, D \succeq 0, \quad (5)$$

where P is orthogonal matrix and D diagonal matrix. This can be rewritten as

$$\Sigma = PDP^T = P \text{diag}(P^T \Sigma P) P^T. \quad (6)$$

To estimate Σ with invertible estimator, first split n observations into two groups of n_1 and $n_2 = n - n_1$ observations. Since we have two groups of observations, we can use the first group of observations to estimate P, and second group of n_2 observations to estimate Σ on the right hand side. Therefore, when we denote the sample covariance matrix of two groups as $S_{n,1}$ and $S_{n,2}$, and \hat{P}_1 the eigenvectors of $S_{n,1}$, proposed estimator is represented as

$$\hat{\Sigma}_{LAM} = \hat{P}_1 \text{diag}(\hat{P}_1^T S_{n,2} \hat{P}_1) \hat{P}_1^T. \quad (7)$$

2.2 Estimation of mean vector

Estimation of the mean vector is another important component of Fisher LDA. In many cases, the estimation of covariance matrix has been focused in high-dimensional discriminant analysis, and the sample mean vector has been commonly used. Shrinkage estimator of mean vector in high dimensional classification has been seriously considered under the assumption that the covariance matrix is a diagonal matrix which is a modified form of the naive Bayes rule. [6] and [2] are representative work applying f -modeling and g -modeling to discriminant analysis under the assumption that all variables are independent.

When we have independent random variables $Y_i \sim N(\mu_i, 1)$ for $1 \leq i \leq p$, a lot of research has been done on the simultaneous estimation of the mean vector, $\mu = (\mu_1, \dots, \mu_p)$. A typical example is the James-Stein estimator, but from a Bayesian point of view, it is an estimator under the assumption that each mean value is generated from a normal distribution, so it has the disadvantage of not reflecting the various structures of the mean values such as bi-modality of mean values which may occur for the case of sparsity of mean values. When p is large, there are two typical methods in nonparametric empirical Bayes methods discussed in [3] : f -modeling based on estimation of marginal density and g -modeling based on estimation of mixing distribution or prior distribution as a non-parametric method. In particular, f -modeling has a simpler calculation process than g -modeling, however with the recent development of various algorithms that can be used for g -modeling, empirical Bayesian methods based on g -modeling are also widely used.

In fact, in the estimation of mean vector, the observed values are assumed to be independent. However, in classification, this assumption is not satisfied in general. Although there exist correlations among all variables, existing studies such as [6] applied NPEB to correlated variables in high dimensional classification problem. Instead, if we can have an estimate of precision matrix or covariance matrix, we can decorrelate the variables through decorrelation based on square root matrix of the estimate of precision matrix.

More specifically, for $p \times p$ positive definite matrix R satisfying $R = \Omega^{1/2}$, we consider

the following decorrelated variables through decorrelation:

$$\mathbf{Z}_i \equiv R\mathbf{X}_i \sim N_p(R\boldsymbol{\mu}_i, R\Sigma R^T) = N(R\boldsymbol{\mu}_i, I_p) \equiv N_p(\boldsymbol{\mu}_i^*, I_p). \quad (8)$$

where $\boldsymbol{\mu}_i = (\mu_{i1}, \dots, \mu_{ip})^T$, $\mathbf{X}_i = (X_{i1}, \dots, X_{ip})^T$ and $\mathbf{Z}_i = (Z_{i1}, \dots, Z_{ip})^T$. Therefore, under these definition, $Z_{ij} \sim N(\mu_{ij}^*, 1)$ are independently distributed. We estimate the mean vector $\boldsymbol{\mu}_i^*$ based on decorrelated observations $\mathbf{Z}_i = (Z_{i1}, \dots, Z_{ip})^T$ and then transform back to $\hat{\boldsymbol{\mu}}_i = R^{-1}\hat{\boldsymbol{\mu}}_i^*$.

NPEB is the mean estimation strategy suggested in [6]. For the random variable Z with variance 1 and its observed value z_1, \dots, z_n , assume hierarchical structure that

$$Z \sim N(M, 1), M \sim G. \quad (9)$$

Here, G is a cumulative distribution function. Under the Bayesian scheme, probability distribution function of Z , g^* , is written as

$$g^*(z) = \int \phi(z - v) dG(v), \quad (10)$$

where $\phi(\cdot)$ is the probability distribution function of standard normal distribution, say $\phi(x) = \exp(-x^2/2)/\sqrt{2\pi}$. Under this distribution, Bayes estimator for μ_i is

$$E(\mu_i|z_i) = z_i + \frac{(g^*)'(z_i)}{g^*(z_i)} \quad (11)$$

where $(g^*)'(z) = \frac{d}{dz}g^*(z)$. The estimates have two categories : one is $\widehat{g^*(z)} = \int \phi(z - v)d\hat{G}(v)$ for some estimate \hat{G} from g -modeling. See [7] and [3]. The other one is g^* is directly estimated from density estimation based on observed values z_1, \dots, z_p , called f -modeling. See [6].

To represent the estimated mean vector using NPEB method, we use the notation of z_{ij}^g to denote the j th element of z_i vector in group g ($i = 1, \dots, n_g$). Let $\bar{z}_j^g = \sum_{k=1}^{n_g} z_{kj}^g/n_g$,

which is the sample mean of j th component in group g . Then $\hat{\mu}_{EB}$ is written elementwise as follows:

$$(\hat{\mu}_{EB})_i = \bar{z}_j^g + \frac{\sum_{j=1}^p (\bar{z}_j^g - \bar{z}_i^g) \phi \{ \sqrt{n_g}(\bar{z}_i^g - \bar{z}_i^g)/h \}}{h^2 \sum_{j=1}^p \phi \{ \sqrt{n_g}(\bar{z}_i^g - \bar{z}_i^g)/h \}}. \quad (12)$$

2.3 Construction of discriminant rules

First, when the prior probability of group 1 and group 2 is provided, the Bayes discriminant rule δ has the form of

$$\delta(\mathbf{x}^{new}) = \left(\mathbf{x}^{new} - \frac{\boldsymbol{\mu}_1 + \boldsymbol{\mu}_2}{2} \right)^\top \boldsymbol{\Sigma}^{-1} (\boldsymbol{\mu}_2 - \boldsymbol{\mu}_1) - \log \frac{p_1}{p_2}, \quad (13)$$

where p_1, p_2 denotes the prior probability of each group. In real data situation, when n_1, n_2 samples are obtained from group 1 and group 2 respectively, prior odds can be replaced to $\frac{n_1}{n_2}$.

When the data is given, we can build a discriminant rule by obtaining the estimates of $\boldsymbol{\Sigma}^{-1}$ and $\boldsymbol{\mu}_1, \boldsymbol{\mu}_2$. In this paper, we first estimate the precision matrix, decorrelate the data, and apply mean vector estimation scheme introduced in the previous section. Assume $\hat{\boldsymbol{\Sigma}}^{-1/2}$ is obtained. Then $\hat{\Omega}^{1/2} \mathbf{X}_{ij} \sim N_p(\hat{\Omega}^{1/2} \boldsymbol{\mu}_j, \hat{\Omega}^{1/2} \Omega^{-1} \hat{\Omega}^{1/2})$ and assuming that $\hat{\Omega}^{1/2}$ estimates Ω properly, $\hat{\Omega}^{1/2} \Omega^{-1} \hat{\Omega}^{1/2}$ can be assumed to be similar to I . Subsequently, we can apply NPEB and NPMLE method under desirable setting, to estimate $\boldsymbol{\Sigma}^{-1/2} \boldsymbol{\mu}_i$.

In each group, we first estimate precision matrix $(\hat{\Omega}_1, \hat{\Omega}_2)$. Then, pool this into one precision matrix using

$$\hat{\boldsymbol{\Sigma}}^{-1} = \hat{\Omega} = \frac{(n_1 - 1)\hat{\Omega}_1 + (n_2 - 1)\hat{\Omega}_2}{n_1 + n_2 - 2}.$$

From this, we obtain the estimate of $\hat{\Omega}^{1/2} \boldsymbol{\mu}_j$ using NPEB and NPMLE method. Let $\boldsymbol{\mu}_j^* = \Omega^{1/2} \boldsymbol{\mu}_j$ and estimated vector to be $\hat{\boldsymbol{\mu}}_j^*$ ($j = 1, 2$). With this procedure, obtained

practical discriminant rule is

$$\delta(x^{new}) = (x^{new} - \frac{\hat{\mu}_1 + \hat{\mu}_2}{2}) \hat{\Sigma}^{-1} (\hat{\mu}_2 - \hat{\mu}_1) - \frac{n_1}{n_2} \quad (14)$$

$$= (\hat{\Sigma}^{-1/2} x^{new} - \frac{\hat{\mu}_1^* + \hat{\mu}_2^*}{2}) (\hat{\mu}_2^* - \hat{\mu}_1^*) - \frac{n_1}{n_2}. \quad (15)$$

Instead of estimating μ_1^* and μ_2^* separately, we can estimate $\mu_2^* - \mu_1^*$ at once using

$$\Omega^{1/2}(\bar{x}_2 - \bar{x}_1) \sim N(\mu_2^* - \mu_1^*, a_n^{-2} I_p),$$

where $a_n = (1/n_1 + 1/n_2)^{-1/2}$ and use sample mean $(\bar{z}_1 + \bar{z}_2)/2$ for $(\hat{\mu}_1^* + \hat{\mu}_2^*)/2$. When we define $\bar{z}_1 = \hat{\Omega}^{1/2} \bar{x}_1$, $\bar{z}_2 = \hat{\Omega}^{1/2} \bar{x}_2$, this discriminant rule is written as

$$\delta(x^{new}) = (x^{new} - \frac{\bar{x}_1 + \bar{x}_2}{2}) \hat{\Sigma}^{-1} (\widehat{\mu_2 - \mu_1}) - \frac{n_1}{n_2} = (\hat{\Sigma}^{-1/2} x^{new} - \frac{\bar{z}_1 + \bar{z}_2}{2}) (\widehat{\mu_2^* - \mu_1^*}) - \frac{n_1}{n_2} \quad (16)$$

where $\widehat{\mu_2^* - \mu_1^*}$ is an estimate of $\mu_2^* - \mu_1^*$. In section 5, we compare (14) and (16)'s performance in real data. We noticed that two discriminant rules show similar performance when same estimation strategies are used. Note that when one estimate μ_1^* , μ_2^* or $\mu_2^* - \mu_1^*$ as a sample mean of corresponding data, (14) and (16) become identical. Therefore, we use the discriminant rule (16) for the simulation and theoretical analysis in section 3. We denote 'NPEB1', 'NPMLE1' for the discriminant rule using NPEB, NPMLE method in (16) and 'NPEB2', 'NPMLE2' for (14).

3 Asymptotic results of the NPEB method

In this section, we present the asymptotic result for the discriminant rule with NPEB method. [9] studied the performance of the discriminant rule with NPMLE in (11) and showed a region for the parameters related to the strength of mean values and the level of sparsity such that

the error rate is asymptotically 0 as dimension increases. We provide an analogous result for NPEB method under the setting in [9] and compare the result with those for NPMLE, hard threshold and naive Bayes rule.

As in [9], we assume that the precision matrix is consistently estimated so that the data are decorrelated in an appropriate way, for example, glasso method provides the uniformly consistent estimators of all components in the precision matrix. We emphasize the effects of mean vector estimations after data are decorrelated.

Under (16), assuming $\Sigma = I_p$ or the precision matrix is consistently estimated, the misclassification error rate of a discriminant rule δ is written as

$$\begin{aligned} P\left(\delta(x^{new}) > 0 \mid x^{new} \in \text{group 2}\right) &= P\left(\left(z^{new} - \frac{\bar{z}_1 + \bar{z}_2}{2}\right)^T \hat{\mu}_D^* > 0 \mid z^{new} \sim N_p(\mu_2^*, I)\right) \\ &= \Phi\left\{-\frac{1}{2}\left(\frac{\mu_D^{*T} \hat{\mu}_D^*}{\|\hat{\mu}_D^*\|_2} + \frac{(\bar{z}_1 + \bar{z}_2 - (\mu_1^* + \mu_2^*))^T \hat{\mu}_D^*}{\|\hat{\mu}_D^*\|_2}\right)\right\}, \end{aligned}$$

where δ is defined in (16), $\mu_D^* = \mu_1^* - \mu_2^*$, $\hat{\mu}_D^* = \widehat{\mu_1^* - \mu_2^*}$. Since

$$\bar{z}_1 + \bar{z}_2 - (\mu_1^* + \mu_2^*) \sim N(0, a_n^{-2} I_p),$$

when n_1 and n_2 are fixed, $\bar{z}_1 + \bar{z}_2 - (\mu_1^* + \mu_2^*) = O_p(1)$. Therefore, from the Cauchy-Schwartz inequality, we have

$$\frac{\{\bar{z}_1 + \bar{z}_2 - (\mu_1^* + \mu_2^*)\}^T \hat{\mu}_D^*}{\|\hat{\mu}_D^*\|_2} = O_p(1).$$

Thus, as $p \rightarrow \infty$, we have the result that $P\left(\delta(x^{new}) > 0 \mid x^{new} \in \text{group 2}\right) \rightarrow 0$ is equivalent to

$$V := \frac{\mu_D^{*T} \hat{\mu}_D^*}{\|\hat{\mu}_D^*\|_2} \xrightarrow{P} \infty. \quad (17)$$

This implies that if $V \xrightarrow{P} \infty$ as $p \rightarrow \infty$, a given decision rule δ has the error rate 0 asymptotically.

[9] derived some conditions under which NPEB, Naive Bayes and hard threshold method achieve (17). For such asymptotic results, the following settings were considered. (17). We

set

$$\mu_D^* = \mu_1^* - \mu_2^* = (p^b, \dots, p^b, 0, \dots, 0), \quad (18)$$

where μ_D^* has $[p^a]$ nonzero elements, where $0 < a < 1$ and $b \in \mathbf{R}$. For simplicity, we define $\Delta = p^b$, $p_1 = [p^a]$.

First, we set $\mu_1 = (0, \dots, 0)$ and $\mu_2 = (\Delta_l^T, \mathbf{0}_{p-l}^T)$ where Δ_l is the l dimensional column vector with all components Δ with

$$\Delta = p^b, l = [p^a] \quad (19)$$

for $b > 0$ and $0 < a < 1$. Δ and l represent the strength of signal for each component and the level of sparsity, respectively. If a discriminant rule has the property of (17) in a wider range of (a, b) than another one, then the first discriminant rule has superiority to the other one. [9] showed that the discriminant rule with NPMLE has advantage over naive Bayes rule and hard threshold in that (17) of NPMLE method is obtained in a wider range than the other two methods.

We derive the range of (a, b) of NPEB and present the following theorem to compare the results of NPMLE, naive Bayes rule and hard threshold method. We denote \mathcal{R}_{NPEB} , \mathcal{R}_{NPMLE} , \mathcal{R}_{SM} and \mathcal{R}_{Hard} as the areas of (a, b) satisfying (17) under the corresponding mean estimation methods. For the illustration of the areas, we define following sets :

$$A = \{(a, b) \in \mathbb{R}^2, 0 \leq a + 2b \leq 1/2 : -0.25 < b < 0 \text{ and } 0 < a < 1\},$$

$$B = \{(a, b) \in \mathbb{R}^2, 3a + 2b \geq 2 : -0.5 < b < 0 \text{ and } 2/3 < a < 1\},$$

$$C = \{(a, b) \in \mathbb{R}^2, a + 2b \leq 1/2 : 0 < b < 0.25 \text{ and } 0 < a < 0.5\},$$

$$D = \{(a, b) \in \mathbb{R}^2, a + 2b \geq 1/2 : -0.25 < b < 0 \text{ and } 0.5 < a < 1\}.$$

Note that when (a, b) satisfies $a + 2b > 1/4$ and $b > 0$, it is known that (17) holds for NPMLE, naive Bayes rule and Hard threshold method (see [9]), however the performance

of the NPEB has not been studied in [9]. We now provide the area of (a, b) of the NPEB satisfying (17) in Theorem 1 and compare those areas.

Theorem 1. *Under (19), we have the following results :*

$$\begin{aligned}\mathcal{R}_{Hard} &= C, \mathcal{R}_{SM} = D, \\ \mathcal{R}_{NPEB} &\supset A \cup C \cup D, \mathcal{R}_{NPMLE} \supset B \cup C.\end{aligned}$$

Proof. See Appendix. □

Note that \mathcal{R}_{NPEB} and \mathcal{R}_{NPMLE} can be enlarged further, while \mathcal{R}_{SM} and \mathcal{R}_{Hard} exactly matches with D and C . The visual illustration of each region is in figure 1.

We can see that NPEB method covers all the area of naive Bayes rule and hard threshold method. On the other hand, neither of NPEB and NPMLE is included in the other method, however both methods are expected to work well in both sparse and dense cases while hard threshold method and naive Bayes rule are designed for only one of sparse and dense cases.

We provide numerical studies in section 4 and 5 to compare these methods, and see that there doesn't seem be any tendency that either of NPMLE and NPEB dominates the other method.

4 Simulations

In this section, we provide simulation results for various combinations of mean vectors and covariance matrices. We divided simulation settings according to the sparseness and denseness of precision matrix and those of the difference of mean vectors.

Under the assumption of multivariate normal distribution, $\Omega_{ij} = 0$ means that X_i and X_j are conditionally independent. To verify the strength of glasso and LAM methods separately, we divided simulation settings according to the sparseness of precision matrix or covariance matrix. To compare mean vector estimation method individually, we assumed the simulation

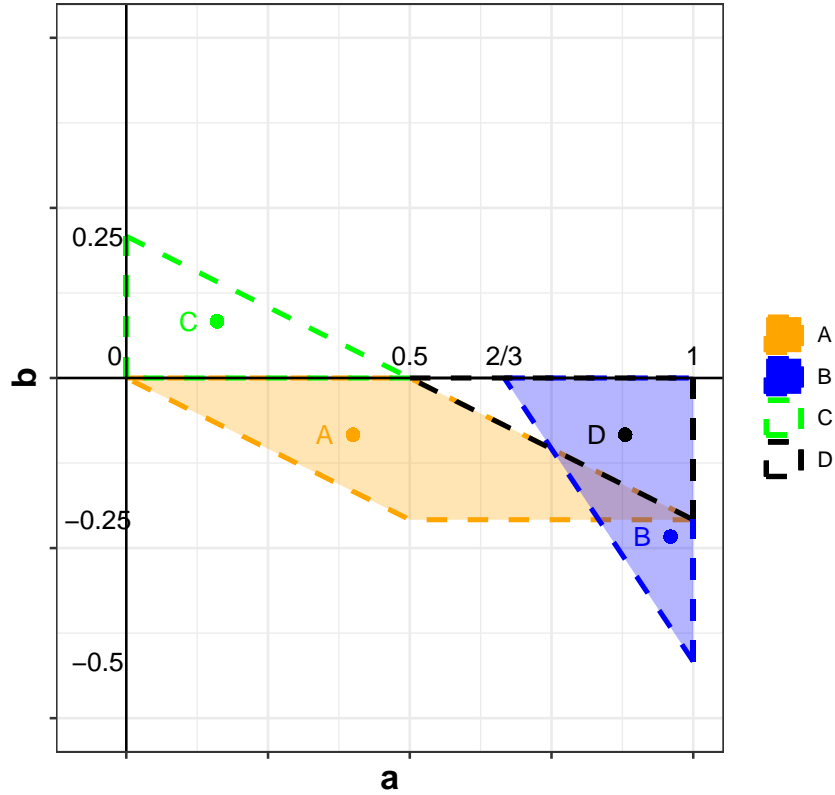


Figure 1: The area of (a, b) under the setting (19)

setting as follows. We set $\mu_1^T = (0, \dots, 0)$, $\mu_2^T = (\Delta_l^T, 0_{p-l}^T)$ where Δ_l is the l dimensional column vector with all component Δ and $\mathbf{0}_{p-l}$ is the $(p - l)$ dimensional vector with all 0 components. In some situation, we set $\mu_{2s} = \Sigma^{1/2} \mu_2 = (\Delta_l^T, \mathbf{0}_{p-l}^T)$. Throughout the simulation, we set $p = 500$ with the number of training data and test data as $n_{1,train} = n_{2,train} = 50$ and $n_{1,test} = n_{2,test} = 250$.

We consider the following simulation settings for various configurations of l and Δ as well as different structure of Σ .

1. Setting 1: AR(1) structured precision matrix. We set Σ^{-1} as $(\Sigma^{-1})_{ij} = \rho^{|i-j|}$.
 - simulation 1-1: $\Delta = 3, l = 20$ in μ_{2s} with $\rho = 0.8$.
 - simulation 1-2: $\Delta = 0.4, l = 400$ in μ_{2s} with $\rho = 0.8$.

2. Setting 2: Blocked AR(1) structured precision matrix. We set Σ^{-1} as $\begin{bmatrix} \Sigma_q^{-1} & 0 \\ 0 & I_{p-q} \end{bmatrix}$, where $(\Sigma_q^{-1})_{ij} = \rho^{|i-j|}$ for $1 \leq i, j \leq q$.
- simulation 2-1: $\Delta = 3, l = 20$ in μ_{2s} with $\rho = 0.9, q = 50$.
- simulation 2-2: $\Delta = 0.15, l = 400$ in μ_{2s} with $\rho = 0.9, q = 50$.
3. Setting 3: Exchangeable precision matrix. We set Σ^{-1} as $(\Sigma^{-1})_{ij}$ to have 1 as a diagonal components and ρ as all off-diagonal elements.
- simulation 3-1: $\Delta = 0.7, l = 20$ in μ_2 with $\rho = 0.3$.
- simulation 3-2: $\Delta = 0.07, l = 20$ in μ_{2s} with $\rho = 0.3$.
4. Setting 4: Toeplitz covariance matrix. We set Σ as $\Sigma_{ij} = 1 / (|i - j| + 1)$.
- simulation 4-1: $\Delta = 1, l = 20$ in μ_2 .
- simulation 4-2: $\Delta = 0.4, l = 20$ in μ_{2s} .
5. Setting 5: Banded covariance matrix. We set Σ as $\Sigma_{ij} = \max(1 - |i - j| / 10, 0)$.
- simulation 5-1: $\Delta = 0.7, l = 20$ in μ_2 .
- simulation 5-2: $\Delta = 0.6, l = 20$ in μ_{2s} .

We present misclassification error rates in table 1 to table 5. We summarize the results as follows :

- Impact of decorrelation of the LAM on the mean vector estimations

From all the results from the LAM and the IR, we noticed that mean vector estimation methods have consistent impact on the error rates. Especially, the SM method is improved by the NPMLE and the NPEB since error rates of the NPEB and the NPMLE methods are smaller than those by the SM.

- Impact of decorrelation using glasso on the mean vector estimations

When the precision matrix is estimated by graphical lasso (glasso), the mean vector

estimation itself didn't show clear impact on the error rate. After applying the NPEB and the NPMLE methods to $\hat{\Omega}^{1/2}(\bar{x}_2 - \bar{x}_1)$, the NPEB and NPMLE methods for the decorrelation from glasso method do not significantly improve the SM with the glasso.

- Impact of glasso and LAM

Depending on the structure of covariance matrix or precision matrix, the glasso and the LAM are designed for sparse and general structures, respectively. For example, in simulation 2-1, the glasso method tends to produce smaller error rates than those from the LAM method. Simulation 2-1 shows the sparse structure of the precision matrix since the AR(1) structure is almost similar to the banded matrix. On the other hand, in situation 3-1 using the precision matrix with all the same off-diagonal terms, the LAM method performs better than glasso method since the precision matrix in simulation 3-1 are considered as dense matrix. These two simulations coincide with the effect of the glasso and the LAM on the different structure of precision matrix such as sparsity and denseness.

- No uniform dominance among precision estimation strategies

Comparing the results in simulation 2-1 and 2-2, one can notice that even though two situations are generated with the same precision matrix, tendency in error rates is dissimilar. In situation 2-1, linear discriminant rule using graphical lasso method shows the lowest error rate with every mean estimation strategy, which is completely opposite to simulation 2-2. Therefore, dominant precision estimation strategy for linear discriminant rule cannot be determined depending on precision matrix only.

- Comparison with theoretical result

The theoretical result can elucidate the significant dominance of the NPMLE and NPEB method over SM method in simulation 1-2 and 2-2 under the IR and LAM method for the estimation of the precision matrix. According to theorem 1, when there is a dense signal with low signal intensity ($5/6 < a < 1, b < 0$), the NPMLE and NPEB methods ensure wider range of b in which the asymptotic error rate is zero

compared to SM method. One can check that simulation 1-2 and 2-2 nearly falls into this area.

- Impact of mean vector estimation by shrinkage

From the results in simulation 3-1 and 3-2, we can observe conspicuous improvements of the SM method in error rates by using the NPMLE and NPEB methods for any given estimation of the precision matrix. When the sparse signals have the intensity which is proportional to the positive power of p , namely, when $0 < a < 1/2$, $0 < b < 1/4$, and $a + 2b < 1/2$ holds, the linear discriminant rules built from the SM method are known to asymptotically act as a random guessing, while the discriminant rules using NPEB and NPMLE have the error rate which asymptotically converges to zero.

5 Real Data Analysis

In this section, we consider five real data sets to compare the performance of various binary classification methods discussed in this paper. Through these real data examples, we investigate the role of mean vector and precision matrix estimation in high-dimensional classification.

Four real datasets are used for comparing performance of discriminant rules.

- EEG data: 122 observations (77: group 1, 45: group 2) with 512 features

We used EEG (Electroencephalography) data to validate linear discriminant rules under multiple estimation methods (which is available at <https://archive.ics.uci.edu/ml/datasets/eeg+database>). The data was initially generated for the large study about genetic predisposition of alcoholism. Measurements from 64 electrodes placed on subject's scalps were sampled at 256 Hz for 1 second. For data pre-processing, we parsed this time series data to 8 intervals and extracted each interval's median value. Therefore, we finally made the data of $64 \times 8 = 512$ dimensional vectors from each subjects. With 122 observations in sum ($n_1 = 77$ subjects from alcoholic group and

	Simulation 1-1				Simulation 1-2			
	Oracle.prec	glasso	LAM	IR	Oracle.prec	glasso	LAM	IR
NPEB1	0.0000 (0.0000)	0.1374 (0.0156)	0.0468 (0.0093)	0.0644 (0.0113)	0.0001 (0.0004)	0.4079 (0.0215)	0.3236 (0.0200)	0.3053 (0.0201)
NPEB2	0.0000 (0.0000)	0.1375 (0.0158)	0.1139 (0.0144)	0.1146 (0.0146)	0.0001 (0.0004)	0.4084 (0.0219)	0.3099 (0.0206)	0.2840 (0.0196)
NPMLE1	0.0000 (0.0000)	0.1370 (0.0157)	0.0324 (0.0078)	0.0520 (0.0101)	0.0000 (0.0000)	0.4073 (0.0217)	0.2288 (0.0183)	0.1422 (0.0162)
NPMLE2	0.0000 (0.0000)	0.1375 (0.0156)	0.0939 (0.0130)	0.0988 (0.0138)	0.0000 (0.0000)	0.4079 (0.0218)	0.1379 (0.0148)	0.0489 (0.0099)
SM	0.0000 (0.0000)	0.1393 (0.0157)	0.1945 (0.0178)	0.1854 (0.0177)	0.0003 (0.0007)	0.4081 (0.0220)	0.4352 (0.0213)	0.4344 (0.0212)

Table 1: Simulation 1 result

	Simulation 2-1				Simulation 2-2			
	Oracle.prec	glasso	LAM	IR	Oracle.prec	glasso	LAM	IR
NPEB1	0.0000 (0.0000)	0.0690 (0.0115)	0.1235 (0.0147)	0.1692 (0.0172)	0.0952 (0.0132)	0.3184 (0.0211)	0.1997 (0.0179)	0.1205 (0.0136)
NPEB2	0.0000 (0.0000)	0.0686 (0.0115)	0.1522 (0.0156)	0.1692 (0.0169)	0.0946 (0.0128)	0.3191 (0.0206)	0.1708 (0.0162)	0.1168 (0.0139)
NPMLE1	0.0000 (0.0000)	0.0687 (0.0116)	0.1199 (0.0148)	0.1609 (0.0164)	0.0868 (0.0126)	0.3196 (0.0211)	0.2036 (0.0167)	0.1112 (0.0139)
NPMLE2	0.0000 (0.0000)	0.0688 (0.0115)	0.1534 (0.0164)	0.1665 (0.0167)	0.0883 (0.0131)	0.3192 (0.0211)	0.2197 (0.0189)	0.1032 (0.0135)
SM	0.0000 (0.0000)	0.0708 (0.0116)	0.1665 (0.0157)	0.2682 (0.0198)	0.2002 (0.0181)	0.3208 (0.0208)	0.2957 (0.0203)	0.2253 (0.0190)

Table 2: Simulation 2 result

	Simulation 3-1				Simulation 3-2			
	Oracle.prec	glasso	LAM	IR	Oracle.prec	glasso	LAM	IR
NPEB1	0.0000 (0.0000)	0.2609 (0.0194)	0.1285 (0.0145)	0.1291 (0.0144)	0.0720 (0.0112)	0.2042 (0.0170)	0.0830 (0.0120)	0.0834 (0.0122)
NPEB2	0.0000 (0.0000)	0.2629 (0.0198)	0.1874 (0.0174)	0.1887 (0.0172)	0.0992 (0.0130)	0.2048 (0.0173)	0.1140 (0.0139)	0.1179 (0.0143)
NPMLE1	0.0000 (0.0000)	0.2611 (0.0196)	0.1130 (0.0137)	0.1154 (0.0142)	0.0648 (0.0110)	0.2047 (0.0168)	0.0724 (0.0113)	0.0728 (0.0114)
NPMLE2	0.0000 (0.0000)	0.2625 (0.0199)	0.1705 (0.0169)	0.1784 (0.0167)	0.0897 (0.0126)	0.2041 (0.0173)	0.1019 (0.0129)	0.1094 (0.0141)
SM	0.0000 (0.0000)	0.2656 (0.0200)	0.2550 (0.0194)	0.2503 (0.0190)	0.1861 (0.0171)	0.2088 (0.0172)	0.1977 (0.0173)	0.1936 (0.0173)

Table 3: Simulation 3 result

	Simulation 4-1				Simulation 4-2			
	Oracle.prec	glasso	LAM	IR	Oracle.prec	glasso	LAM	IR
NPEB1	0.1888 (0.0172)	0.1990 (0.0178)	0.1554 (0.0155)	0.1625 (0.0159)	0.2601 (0.0198)	0.2523 (0.0190)	0.2024 (0.0171)	0.2107 (0.0176)
NPEB2	0.2424 (0.0185)	0.1985 (0.0177)	0.1612 (0.0164)	0.1684 (0.0168)	0.3314 (0.0212)	0.2527 (0.0192)	0.2150 (0.0180)	0.2191 (0.0184)
NPMLE1	0.1691 (0.0159)	0.1983 (0.0178)	0.1536 (0.0155)	0.1610 (0.0162)	0.2385 (0.0187)	0.2524 (0.0191)	0.2020 (0.0175)	0.1610 (0.0162)
NPMLE2	0.2241 (0.0182)	0.1985 (0.0176)	0.1579 (0.0161)	0.1666 (0.0167)	0.3215 (0.0217)	0.2530 (0.0192)	0.2127 (0.0185)	0.1666 (0.0167)
SM	0.2998 (0.0208)	0.2015 (0.0180)	0.1944 (0.0172)	0.1919 (0.0169)	0.3660 (0.0217)	0.2558 (0.0192)	0.2448 (0.0187)	0.2422 (0.0190)

Table 4: Simulation 4 result

	Simulation 5-1				Simulation 5-2			
	Oracle.prec	glasso	LAM	IR	Oracle.prec	glasso	LAM	IR
NPEB1	0.0960 (0.0134)	0.3562 (0.0209)	0.3077 (0.0203)	0.3055 (0.0215)	0.1164 (0.0144)	0.1346 (0.0147)	0.1060 (0.0133)	0.1004 (0.0131)
NPEB2	0.1250 (0.0146)	0.3592 (0.0207)	0.3224 (0.0211)	0.3190 (0.0212)	0.1732 (0.0165)	0.1363 (0.0149)	0.1124 (0.0134)	0.1026 (0.0135)
NPMLE1	0.0926 (0.0130)	0.3559 (0.0212)	0.3059 (0.0203)	0.3005 (0.0210)	0.1040 (0.0131)	0.1341 (0.0147)	0.1045 (0.0133)	0.0992 (0.0130)
NPMLE2	0.1131 (0.0143)	0.3579 (0.0207)	0.3206 (0.0209)	0.3135 (0.0207)	0.1611 (0.0159)	0.1358 (0.0150)	0.1112 (0.0134)	0.1019 (0.0133)
SM	0.2020 (0.0174)	0.3633 (0.0212)	0.3667 (0.0207)	0.3464 (0.0216)	0.2451 (0.0194)	0.1397 (0.0152)	0.1377 (0.0151)	0.1166 (0.0139)

Table 5: Simulation 5 result

$n_2 = 45$ from control group), we examined the performance of each discriminant rule using LOOCV method.

- Gravier data: 168 observations (111: group 1, 57: group 2) with 1000 features

Gene array data obtained for the study pertaining to the prediction of metastasis of small node-negative breast carcinoma is also utilized, which we named Gravier data. Small invasive ductal carcinomas without axillary lymph node involvement (T1T2N0) were analyzed from 168 patients. Among these, 111 subjects who had no events for 5 years afterwards were categorized as group 1, and other 57 subjects with early metastasis were assigned as group 2. We processed the original data by extracting 1000 features which have the most significant t values among the 2905 features beforehand.

- Ham data : 214 observations (111: group 1, 103: group 2) with 431 features.

Ham data was obtained by food spectrograph about 19 Spanish and 18 French dry-cured hams. Food spectrograph is utilized in chemometrics to classify food types, which can be directly used to assure food safety and quality. This data is publicly available at <http://www.timeseriesclassification.com/description.php?Dataset=Ham>. From in total 37 hams, up to 6 observations were obtained. Therefore, 214 observations were categorized into two groups (111 observations for group 1 and 103 for group 2), with 431 feature vectors for each observations. Data preprocessing procedure is described in ‘Sodium dodecyl sulphate-polyacrylamide gel electrophoresis of proteins in dry-cured hams: Data registration and multivariate analysis across multiple gels’ (to be in reference).

- IMVigor data: 298 observations (230: group 1, 68: group 2) with 4792 features (divided into 7 groups)

Clinical outcome of metastatic unorthelial cancer patients were collected from (IMVigor reference here). Observations about 230 non-responders and 68 responders are composed of 4792 feature vectors. These features are known to be correlated within seven groups, which contains 1583, 975, 569, 548, 546, 341, 230 features each. Therefore,

we investigated the error rate of linear discriminant rules with and without this group information.

Within these data, classification performance has been measured through Leave-One-Out Cross Validation (LOOCV) method. As introduced in 2.3, linear discriminant rules can be constructed by estimating μ_1^* and μ_2^* respectively, or $\mu_2^* - \mu_1^*$ at once. Therefore, we compared the error rate of each discriminant rule according to mean estimation method, precision estimation method, and discriminant rule construction method.

As one can see from table 6, classification errors largely depend on precision matrix estimation methods. More suitable precision estimation method relies on the data. For example, in HAM data, LAM method shows lower error rate while glasso method performs well with Gravier data. Among mean vector estimation methods, error rates does not vary significantly. However, when classifying Gravier data with glasso precision estimation method, error rate varied significantly according to mean estimation method. Therefore, we compared each component of $\widehat{\mu_2^* - \mu_1^*} = \widehat{\Sigma}^{-1/2} \widehat{\mu_2 - \mu_1}$ among mean estimation methods.

Figure 2 shows the plots of NPEB vs. SM and NPMLE vs. SM after two methods of decorrelation. The NPEB and NPMLE tend to have the effect of shrinkage of SM especially for large values of SM. It is seen that the NPMLE in (11) with the estimated \hat{G} has the monotonicity property of SM. On the other hand, the NPEB with estimated marginal density \hat{f} and \hat{f}' is not guaranteed to have the monotonicity, so there exists some wiggly patterns in local regions, however overall patterns of NPEB are similar to those of NPMLE.

To summarize, the decorrelation such as glasso and LAM methods is effective in most of cases in that the IR without decorrelation is improved although those two methods make the IR worse in some data sets. In particular, the glasso is sensitive to different cases since the glasso is designed for sparse structured precision matrix. On the other hand, the LAM method is robust to all data sets except Gravier data in which the performance of all classification methods are worse than the glasso and the IR. For the glasso method, different classification methods have large variations in error rate while the LAM method produce quite similar error rates for different rules.

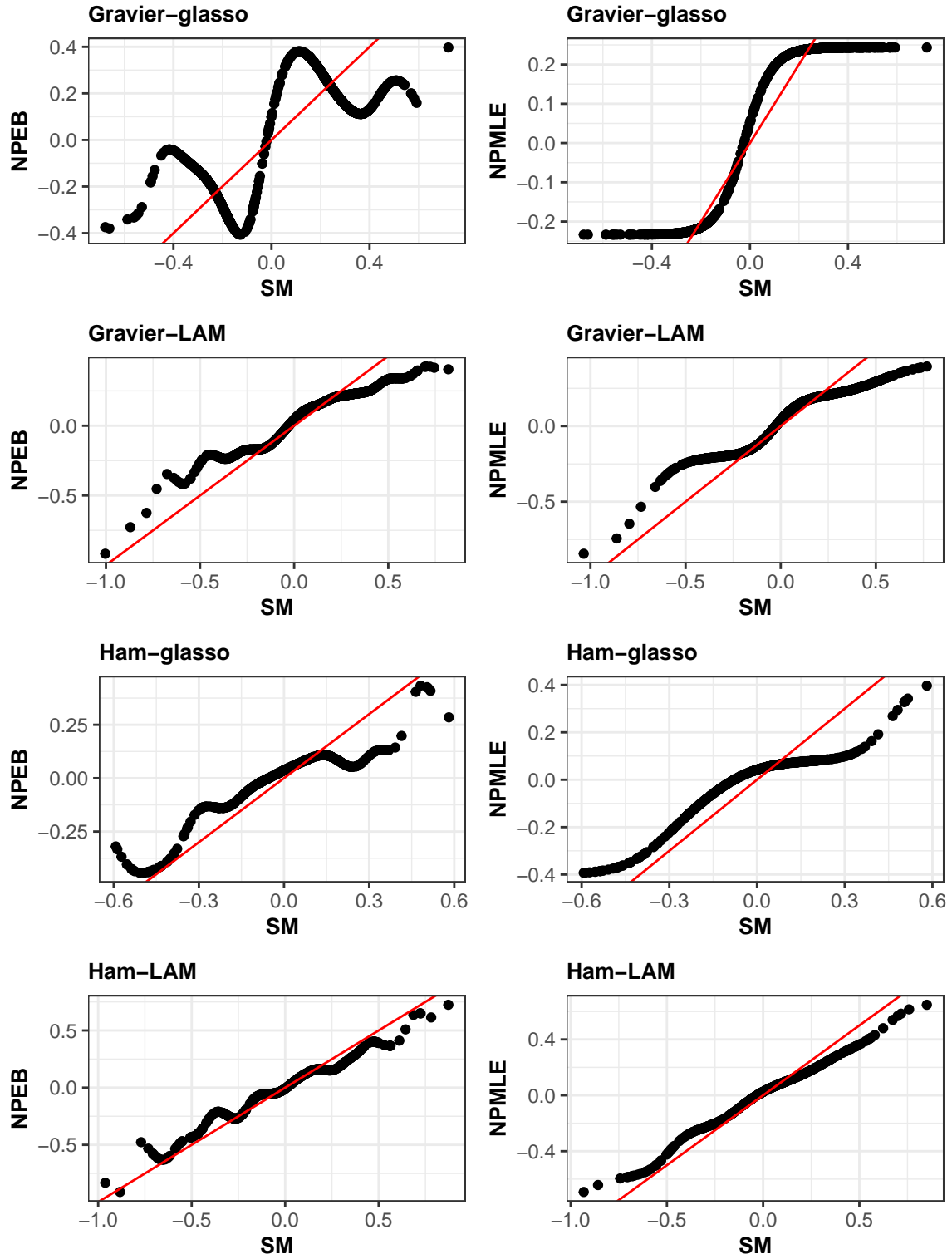


Figure 2: $(\widehat{\mu}_2^* - \widehat{\mu}_1^*)$ plot - NPEB, NPMLE method to SM method

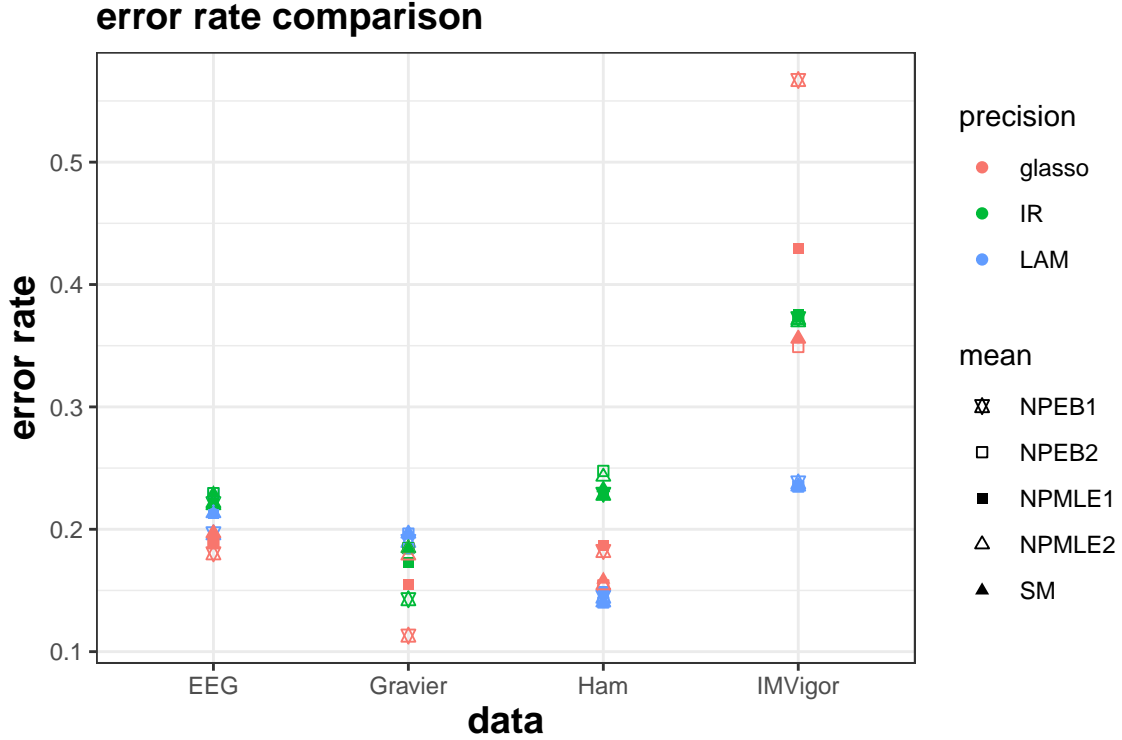


Figure 3: Error rate comparison according to mean and precision estimation methods

	EEG			Gravier			Ham			IMVigor		
	glasso	LAM	IR	glasso	LAM	IR	glasso	LAM	IR	glasso	LAM	IR
NPEB1	*22/122	24/122	27/122	*19/168	32/168	24/168	39/214	31/214	49/214	169/298	71/298	111/298
NPEB2	23/122	28/122	28/122	31/168	33/168	31/168	33/214	*30/214	53/214	104/298	*70/298	111/298
NPMLE1	23/122	26/122	27/122	26/168	31/168	29/168	40/214	32/214	49/214	128/298	*70/298	112/298
NPMLE2	24/122	26/122	27/122	30/168	33/168	31/168	33/214	*30/214	52/214	106/298	*70/298	110/298
SM	24/122	26/122	28/122	31/168	33/168	31/168	34/214	*30/214	50/214	106/298	*70/298	111/298

Table 6: LOOCV classification result about EEG, Gravier, Ham, and IMVigor datasets of corresponding discriminant rules. '*' indicates the lowest error rate in each data set.

6 Concluding Remarks

Combining different types of the precision matrix and mean vector estimation strategies, we investigate the performances of the various linear discriminant rules. We evaluate these rules

under various contrived settings, with dense and sparse structures of precision matrices and the difference of mean vectors, the performances of the discriminant rules are investigated. We therefore observe that linear discriminant rules perform well when the simulation situation is aligned with the assumptions that each estimation strategies are based on. Our results including numerical studies and real data examples show that none of the discriminant rules tend to dominate the others. In particular, we emphasize that the theoretical result is presented on the NPEB. We believe that this is an interesting result in the sense that we can compare f -modeling and g -modeling theoretically which are corresponding to the NPEB and NPMLE where the performance of the NPMLE is studied in [9].

One interesting phenomenon is that the structure of mean vector may be changed after decorrelation. Since our results in this paper show that the different methods of estimation of mean vectors have different performances depending on the structure of mean vectors, so it will be interesting to investigate the changes of mean vector structures after decorrelation and their effect on the choice of estimation methods. We leave this as a future work.

Acknowledgement

Research of J. Park was supported by the National Research Foundation of Korea (NRF) grant funded by the Korea government (MSIT) (No. 2020R1A2C1A01100526).

References

- [1] BROWN, L. D., AND GREENSHTEIN, E. Nonparametric empirical bayes and compound decision approaches to estimation of a high-dimensional vector of normal means. *The Annals of Statistics* (2009), 1685–1704.
- [2] DICKER, L. H., AND ZHAO, S. D. Nonparametric empirical bayes and maximum likelihood estimation for high-dimensional data analysis. *arXiv preprint arXiv:1407.2635* (2014).

- [3] EFRON, B. Two modeling strategies for empirical bayes estimation. *Statistical science: a review journal of the Institute of Mathematical Statistics* 29, 2 (2014), 285.
- [4] FAN, J., AND FAN, Y. High dimensional classification using features annealed independence rules. *Annals of statistics* 36, 6 (2008), 2605.
- [5] FRIEDMAN, J., HASTIE, T., AND TIBSHIRANI, R. Sparse inverse covariance estimation with the graphical lasso. *Biostatistics* 9, 3 (2008), 432–441.
- [6] GREENSHTEIN, E., AND PARK, J. Application of non parametric empirical bayes estimation to high dimensional classification. *Journal of Machine Learning Research* 10, 7 (2009).
- [7] JIANG, W., AND ZHANG, C.-H. General maximum likelihood empirical bayes estimation of normal means. *The Annals of Statistics* 37, 4 (2009), 1647–1684.
- [8] LAM, C. Nonparametric eigenvalue-regularized precision or covariance matrix estimator. *The Annals of Statistics* 44, 3 (2016), 928–953.
- [9] PARK, H., BAEK, S., AND PARK, J. High-dimensional linear discriminant analysis using nonparametric methods. *Journal of Multivariate Analysis* 188 (2022), 104836.

A Proof of Theorem 1

We define $\bar{z}_D = \bar{z}_1 - \bar{z}_2$ which has $\bar{z}_D \sim N(\mu_D^*, a_n^{-2}I_p)$ where $a_n = (1/n_1 + 1/n_2)^{-1/2}$. From (12), the estimator using EB method of mean difference μ_D^* is as follows:

$$\widehat{\mu}_{D,i}^{EB} = \bar{z}_{D,i} + \frac{1}{h^2} \frac{\sum_{j=1}^p (\bar{z}_{D,j} - \bar{z}_{D,i}) \phi \left\{ \frac{a_n(\bar{z}_{D,i} - \bar{z}_{D,j})}{h} \right\}}{\sum_{j=1}^p \phi \left\{ \frac{a_n(\bar{z}_{D,i} - \bar{z}_{D,j})}{h} \right\}}. \quad (20)$$

$\widehat{\mu}_{D,i}^{EB}$ denotes the i -th component of the EB estimator of the mean vector $\widehat{\mu}_D^{EB}$ and $\bar{z}_{D,i}$ is that of \bar{z}_D . Here, $\phi(\cdot)$ is the probability distribution function of standard Gaussian distribution. According to [1] and [6], we choose the bandwidth $h = 1/\sqrt{\log p}$ in (20).

Since $\bar{z}_D \sim N(\mu_D^*, a_n^{-2}I_p)$, we have $\bar{z}_{D,i} \sim N(\mu_i^*, a_n^{-2})$ which are mutually independent. Thus, we can rewrite $\bar{z}_{D,i}$ as follows using independent $S_i \sim N(0, 1)$ for $1 \leq i \leq p$:

$$\bar{z}_{D,i} = \begin{cases} \Delta + S_i/a_n, & \text{if } i = 1, \dots, p_1 \\ S_i/a_n, & \text{if } i = p_1 + 1, \dots, p. \end{cases}$$

For the simplicity in notation, we define the followings :

$$S_{ij}^- = S_i - S_j, \quad S_i^* = S_i + a_n\Delta, \quad (21)$$

$$T_i = \exp \left\{ -\frac{S_i^2}{2(1+h^2)} \right\}, \quad T_i^* = \exp \left\{ -\frac{S_i^{*2}}{2(1+h^2)} \right\}. \quad (22)$$

With these notations, $\widehat{\mu}_{D,i}^{EB}$ is represented as

$$\widehat{\mu}_{D,i}^{EB} = \begin{cases} \Delta + \frac{S_i}{a_n} + \frac{\sum_{j=1}^{p_1} \frac{S_{ji}^-}{a_n} \phi(S_{ij}^-/h) + \sum_{j=p_1+1}^p \frac{S_{ji}^- - a_n\Delta}{a_n} \phi\{(S_{ij}^- + a_n\Delta)/h\}}{h^2 \left[\sum_{j=1}^{p_1} \phi(S_{ij}^-/h) + \sum_{j=p_1+1}^p \phi\{(S_{ij}^- + a_n\Delta)/h\} \right]}, & \text{if } i \leq p_1 \\ \frac{S_i}{a_n} + \frac{\sum_{j=1}^{p_1} \frac{S_{ji}^- + a_n\Delta}{a_n} \phi\{(S_{ij}^- - a_n\Delta)/h\} + \sum_{j=p_1+1}^p \frac{S_{ji}^-}{a_n} \phi(S_{ij}^-/h)}{h^2 \left[\sum_{j=1}^{p_1} \phi\{(S_{ij}^- - a_n\Delta)/h\} + \sum_{j=p_1+1}^p \phi(S_{ij}^-/h) \right]}, & \text{o.w.} \end{cases} \quad (23)$$

We now show that, for $(a, b) \in \mathcal{R}_{NP\text{EB}}$ defined in section 3, we have the divergence of V in probability as in (17).

For this, we consider two cases depending on the sign of b : (i) $b < 0$ and (ii) $b > 0$.

the proof for $A \cup D \subset \mathcal{R}_{NPEB}$

In this case, we provide the proof of $\mathcal{R}_{NPEB} \supset A \cup D$, in which (a, b) satisfies $a + 2b > 0$ and $-1/4 < b < 0$. For the proof of (17), we have the following roadmap consisting of two steps :

Step 1 : we present a lower bound of the numerator in V such as

$$\widehat{\mu_D^*}^T \mu_D^* \geq \frac{h^2}{1 + h^2} a_n p^{a+2b} \{1 + o_p(1)\}.$$

Step 2 : an upper bound of the denominator in V ,

$$\|\widehat{\mu_D^*}\|_2 = O_p \left\{ p^{\max(2a+2b-1, \epsilon')} \right\}.$$

We present the proofs of (i) Step 1 and (ii) Step 2 as follows.

Step 1 : From the definition of $\widehat{\mu_{D,i}^{EB}}$ in (23), one can observe that

$$\widehat{\mu_{D,i}^{EB}} \equiv \Delta + \frac{S_i}{a_n} + \frac{1}{h^2} \left(\sum_{j=1}^{p_1} w_j \frac{S_{ji}^-}{a_n} + \sum_{j=p_1+1}^p w_j \frac{S_{ji}^- - a_n \Delta}{a_n} \right) \quad (24)$$

for $1 \leq i \leq p_1$ where $\sum_{j=1}^p w_j = 1$ with

$$w_j = \phi(S_{ij}^-/h) / \left[\sum_{j=1}^{p_1} \phi(S_{ij}^-/h) + \sum_{j=p_1+1}^p \phi\{(S_{ij}^- + a_n \Delta)/h\} \right] \quad (25)$$

for $1 \leq j \leq p_1$ and

$$w_j = \phi\{(S_{ij}^- + a_n \Delta)/h\} / \left[\sum_{j=1}^{p_1} \phi(S_{ij}^-/h) + \sum_{j=p_1+1}^p \phi\{(S_{ij}^- + a_n \Delta)/h\} \right] \quad (26)$$

for $p_1 + 1 \leq j \leq p$. From (24), one can check that

$$\widehat{\mu}_{D,i}^{EB} \geq \Delta + \frac{S_i}{a_n} + \frac{1}{a_n h^2} \min \{(S_{ji}^-)_{1 \leq j \leq p_1}, (S_{ji}^- + a_n \Delta)_{p_1+1 \leq j \leq p}\} \quad (27)$$

always holds for $1 \leq i \leq p_1$ since the weighted mean is always greater than the minimum value.

Subsequently, we define A_i, B_i, C_i, D_i as follows:

$$A_i = \sum_{j=1}^{p_1} \frac{S_{ji}^-}{a_n} \phi(S_{ij}^-/h) \equiv \sum_{j=1}^{p_1} w_{1j} \frac{S_{ji}^-}{a_n}, \quad (28)$$

$$B_i = \sum_{j=p_1+1}^p \phi\{(S_{ij}^- + a_n \Delta)/h\} \frac{S_{ji}^- - a_n \Delta}{a_n} \equiv \sum_{j=1}^{p_1} w_{2j} \frac{S_{ji}^- - a_n \Delta}{a_n}, \quad (29)$$

$$C_i = \sum_{j=1}^{p_1} \phi(S_{ij}^-/h) \equiv \sum_{j=1}^{p_1} w_{1j}, \quad (30)$$

$$D_i = \sum_{j=p_1+1}^p \phi\{(S_{ij}^- + a_n \Delta)/h\} \equiv \sum_{j=p_1+1}^p w_{2j}. \quad (31)$$

For independent S_i and S_j following $N(0, 1)$, one can check

$$E \left[\phi(S_{ji}^-/h) \mid S_i \right] = \frac{h}{\sqrt{2\pi}\sqrt{1+h^2}} T_i, \quad (32)$$

$$E \left[S_{ij}^- \phi(S_{ji}^-/h) \mid S_i \right] = -\frac{h^3}{\sqrt{2\pi}\sqrt{1+h^2}^3} S_i T_i. \quad (33)$$

Similar relation holds for S_i^* and T_i^* as follows.

$$E \left[\phi\{(S_{ji}^- - a_n \Delta)/h\} \mid S_i^* \right] = \frac{h}{\sqrt{2\pi}\sqrt{1+h^2}} T_i^*, \quad (34)$$

$$E \left[(S_{ij}^- + a_n \Delta) \phi \left\{ (S_{ji}^- - a_n \Delta)/h \right\} \middle| S_i^* \right] = -\frac{h^3}{\sqrt{2\pi}\sqrt{1+h^2}^3} S_i^* T_i^*. \quad (35)$$

In addition, using the fact that $\phi(x)$ is bounded from 0 to $1/\sqrt{2\pi}$, we obtain the following result : for given T_i , S_{ij}^- are independent for $1 \leq j \leq p_1$ conditioning on S_i , therefore, by Hoeffding's inequality, we have

$$P \left(\left| C_i - \frac{1}{\sqrt{2\pi}} - \frac{(p_1 - 1)h}{\sqrt{2\pi}\sqrt{1+h^2}} T_i \right| > p_1^{1/2+\epsilon} \middle| S_i \right) \leq 2 \exp(-4\pi(p_1 - 1)^{2\epsilon}) \quad (36)$$

since

$$E [C_i | T_i] = E \left[\sum_{j=1}^{p_1} \phi (S_{ij}^-/h) \middle| T_i \right] = \frac{1}{\sqrt{2\pi}} + \frac{(p_1 - 1)h}{\sqrt{2\pi}\sqrt{1+h^2}} T_i.$$

By taking expectation of S_i in (36), we have

$$P \left(\left| C_i - \frac{1}{\sqrt{2\pi}} - \frac{(p_1 - 1)h}{\sqrt{2\pi}\sqrt{1+h^2}} T_i \right| > p_1^{1/2+\epsilon} \right) \leq 2 \exp \{ -4\pi(p_1 - 1)^{2\epsilon} \}. \quad (37)$$

With similar procedures, we also have

$$P \left(\left| D_i - \frac{(p - p_1)h}{\sqrt{2\pi}\sqrt{1+h^2}} T_i^* \right| > (p - p_1)^{1/2+\epsilon} \right) \leq 2 \exp \{ -4\pi(p - p_1)^{2\epsilon} \}. \quad (38)$$

and, from the bound of $x\phi(x)$, we obtain

$$P \left(\left| A_i + \frac{(p_1 - 1)h^3 S_i}{\sqrt{2\pi}\sqrt{1+h^2}^3} T_i \right| > p_1^{1/2+\epsilon} \right) \leq 2 \exp \{ -\pi e (p_1 - 1)^{2\epsilon} \log p \},$$

$$P \left(\left| B_i + \frac{(p - p_1)h^3 S_i^*}{\sqrt{2\pi}\sqrt{1+h^2}^3} T_i^* \right| > (p - p_1)^{1/2+\epsilon} \right) \leq 2 \exp \{ -\pi e (p - p_1)^{2\epsilon} \log p \}.$$

We define the events E_{1i}, \dots, E_{5i} as follows:

$$\begin{aligned}
E_{1i} &= \left\{ \left| A_i + \frac{(p_1 - 1)h^3 S_i}{\sqrt{2\pi}\sqrt{1 + h^2}^3} T_i \right| < p_1^{1/2+\epsilon} \right\}, \\
E_{2i} &= \left\{ \left| B_i + \frac{(p - p_1)h^3 S_i^*}{\sqrt{2\pi}\sqrt{1 + h^2}^3} T_i^* \right| < (p - p_1)^{1/2+\epsilon} \right\}, \\
E_{3i} &= \left\{ \left| C_i - \frac{1}{\sqrt{2\pi}} - \frac{(p_1 - 1)h}{\sqrt{2\pi}\sqrt{1 + h^2}} T_i \right| < p_1^{1/2+\epsilon} \right\}, \\
E_{4i} &= \left\{ \left| D_i - \frac{(p - p_1)h}{\sqrt{2\pi}\sqrt{1 + h^2}} T_i^* \right| < (p - p_1)^{1/2+\epsilon} \right\}, \\
E_{5i} &= \left\{ \max_{1 \leq j \leq p} |S_j| + a_n \Delta < \log p \right\}.
\end{aligned}$$

Let $E_i = \cap_{j=1}^5 E_{ji}$. Applying Bonferroni's inequality on E_i^c and from (53), we obtain

$$\begin{aligned}
P(E_i) &= 1 - P(E_i^c) = 1 - P(\cup_{j=1}^5 E_{ji}^c) \\
&\geq 1 - \sum_{j=1}^5 P(E_{ji}^c) \\
&= 1 - 8 \exp \{ -\pi e (p_1 - 1)^{2\epsilon} \} - 1/p.
\end{aligned}$$

Therefore, when we define $E = \cap_{i=1}^{p_1} E_i$, we have

$$P(E) = 1 - P(E^c) = 1 - P(\cup_{i=1}^{p_1} E_i^c) \tag{39}$$

$$\geq 1 - \sum_{i=1}^{p_1} \{1 - P(E_i)\} \tag{40}$$

$$\geq 1 - 8p_1 \exp \{ -\pi e (p_1 - 1)^{2\epsilon} \} - 1/p^{1-a} \tag{41}$$

Note that for all $0 < a < 1$, $\lim_{p \rightarrow \infty} P(E) = 1$. On the event E , we can set the bounds for A_i, B_i, C_i, D_i to eventually build a lower bound of $\widehat{\mu}_{D,i}^{EB}$. Since $\lim_{p \rightarrow \infty} P(E) = 1$, our aim is to define an appropriate lower bound, W_i , on E which satisfies

$$V = \frac{\widehat{\mu}_D^* \mu_D^*}{\|\widehat{\mu}_D^*\|_2} = \frac{\Delta \sum_{i=1}^{p_1} \widehat{\mu}_{D,i}^{EB}}{\|\widehat{\mu}_D^*\|_2} \geq \frac{\Delta \sum_{i=1}^{p_1} W_i}{\|\widehat{\mu}_D^*\|_2} \xrightarrow{p} \infty. \quad (42)$$

for $(a, b) \in \mathcal{R}_{NPEB}$.

We apply the result in Lemma 4 and obtain $\Delta \sum_{i=1}^{p_1} \widehat{\mu}_{D,i}^{EB} \geq \Delta \sum_{i=1}^{p_1} W_i$ where W_i is defined in Lemma 4 which leads to

$$\widehat{\mu}_D^* \mu_D^* = \Delta \sum_{i=1}^{p_1} \widehat{\mu}_{D,i}^{EB} \geq \Delta \sum_{i=1}^{p_1} W_i \geq \frac{h^2}{1+h^2} a_n p^{a+2b} \{1 + o_p(1)\}. \quad (43)$$

This inequality holds on E , and E has the probability larger than $1 - 8p_1 \exp\{-\pi e(p_1 - 1)^{2\epsilon}\} - p^{-1+a}$, which goes to 1 for all $0 < a < 1$ as $p \rightarrow \infty$.

Step 2 : The denominator in (17) can be bounded using the result obtained in [1] (equation 45). For $\nu = 1 + h^2$, when

$$\begin{aligned} \delta_i &:= \frac{\sum_{j=1}^{p_1} \Delta \phi \{(a_n \bar{z}_{D,i} - a_n \Delta) / \sqrt{\nu}\}}{\sum_{j=1}^{p_1} \phi \{(a_n \bar{z}_{D,i} - a_n \Delta) / \sqrt{\nu}\} + \sum_{j=p_1+1}^p \phi \{(a_n \bar{z}_{D,i} - a_n \Delta) / \sqrt{\nu}\}} \\ &= \begin{cases} \frac{p_1 \Delta \phi \{(S_i - a_n \Delta) / \sqrt{\nu}\}}{p_1 \phi \{(S_i - a_n \Delta) / \sqrt{\nu}\} + (p - p_1) \phi \{(S_i - a_n \Delta) / \sqrt{\nu}\}}, & \text{if } i \leq p_1 \\ \frac{p_1 \Delta \phi \{(a_n \Delta + S_i) / \sqrt{\nu}\}}{p_1 \phi \{(a_n \Delta + S_i) / \sqrt{\nu}\} + (p - p_1) \phi \{(a_n \Delta + S_i) / \sqrt{\nu}\}}, & \text{o.w} \end{cases}, \end{aligned}$$

$$E \left[\sum_{i=1}^p (\delta_i - \widehat{\mu}_{D,i}^{EB})^2 \right] = o(p^\epsilon) \quad (44)$$

holds for all $\epsilon > 0$.

Using this, one obtain the probabilistic upper bound of $\|\widehat{\mu}_D^{EB}\|_2^2$ from

$$\|\widehat{\mu}_D^{EB}\|_2^2 \leq 2 \sum_{i=1}^p (\delta_i - \widehat{\mu}_{D,i}^{EB})^2 + 2 \sum_{i=1}^p \delta_i^2. \quad (45)$$

Since S_i are i.i.d., $E \left[\sum_{i=1}^p \delta_i^2 \right]$ is simplified as follows :

$$\begin{aligned} E \left[\sum_{i=1}^p \delta_i^2 \right] &= p_1 E \left[\frac{p_1 \Delta \phi(S_i/\sqrt{\nu})}{p_1 \phi(S_i/\sqrt{\nu}) + (p-p_1) \phi\{(a_n \Delta + S_i)/\sqrt{\nu}\}} \right]^2 \\ &\quad + (p-p_1) E \left[\frac{p_1 \Delta \phi\{(S_i - a_n \Delta)/\sqrt{\nu}\}}{p_1 \phi\{(S_i - a_n \Delta)/\sqrt{\nu}\} + (p-p_1) \phi(S_i/\sqrt{\nu})} \right]^2 \\ &= p_1 E \left[\frac{p_1 \Delta}{p_1 + (p-p_1) \exp\{-a_n \Delta(a_n \Delta + 2S_i)/(2\nu)\}} \right]^2 \\ &\quad + (p-p_1) E \left[\frac{p_1 \Delta \exp\{-a_n \Delta(a_n \Delta - 2S_i)/(2\nu)\}}{p_1 \exp[-a_n \Delta(a_n \Delta - 2S_i)/(2\nu)] + (p-p_1)} \right]^2 \\ &=: J_1 + J_2. \end{aligned}$$

From $e^{-x} \geq 1 - x$ for all x , under the event E , J_1 and J_2 satisfy

$$J_1 \leq p_1 \left\{ \frac{p_1 \Delta}{p - (p-p_1)a_n \Delta(a_n \Delta + 2 \log p)/2} \right\}^2, \quad J_2 \leq (p-p_1) \left\{ \frac{p_1 \Delta}{p_1 + (p-p_1)} \right\}^2,$$

which implies $E \left[\sum_{i=1}^p \delta_i^2 \right] \leq p^{2a+2b-1} \{1 + o(1)\}$. As a result, from (44) and (45), we have

$$\|\widehat{\mu}_D^{EB}\|_2^2 = O_p \left\{ p^{\max(2a+2b-1, \epsilon')} \right\} \quad (46)$$

for all $\epsilon' > 0$.

Therefore, we prove the results in *Step 1 and Step 2* leading to

$$V = \frac{\widehat{\mu}_D^{*T} \mu_D^*}{\|\widehat{\mu}_D^*\|_2} \geq \frac{\frac{h^2}{1+h^2} a_n p^{a+2b} (1 + o_p(1))}{\sqrt{p^{\max(2a+2b-1, \epsilon')}} O_p(1)} \quad (47)$$

$$= \frac{a_n}{\log p} p^{a+2b - \max(a+b-1/2, \epsilon'/2)} \frac{1 + o_p(1)}{\sqrt{O_p(1)}} \xrightarrow{P} \infty \quad (48)$$

for $-1/4 < b < 0$ and $a + 2b > \epsilon'/2$ since $a + 2b - \max(a + b - 1/2, \epsilon'/2) > 0$ for the given region of (a, b) .

the proof for $C \subset \mathcal{R}_{NPEB}$

Here, we show that (17) is satisfied for all (a, b) with $b > 0$. Since $\widehat{\mu}_D^{*T} \mu_D^* = \Delta \sum_{i=1}^{p_1} \widehat{\mu}_{D,i}^{EB}$ and $\widehat{\mu}_{D,i}^{EB} \geq Z_{2i}$ always holds,

$$\widehat{\mu}_D^{*T} \mu_D^* \geq \Delta \left(\sum_{i=1}^{p_1} \left[\Delta + \frac{1}{a_n} S_i + \frac{1}{a_n h^2} \min \{ (S_{ji}^-)_{1 \leq j \leq p_1}, (S_{ji}^- + a_n \Delta)_{p_1+1 \leq j \leq p} \} \right] \right) \quad (49)$$

$$\geq \Delta \left[\sum_{i=1}^{p_1} \left\{ \Delta + \left(\frac{1}{a_n} - \frac{1}{a_n h^2} \right) S_i - \frac{1}{a_n h^2} \min_{1 \leq j \leq p} S_j \right\} \right]. \quad (50)$$

Therefore, from lemma 2 and the central limit theorem, one can obtain $\widehat{\mu}_D^{*T} \mu_D^* \geq p^{a+2b} \{1 + o_p(1)\}$.

In addition, by using $E[\exp(AS_i)] = \exp(A^2/2)$ for $S_i \sim N(0, 1)$, we have

$$\begin{aligned} E \sum_{i=1}^p \delta_i^2 &\leq p_1 \Delta^2 + (p - p_1) E \left[\frac{p_1 \Delta \exp \{ -a_n \Delta (a_n \Delta - 2S_i) / (2\nu) \}}{p - p_1} \right]^2 \\ &\leq p^{a+2b} + \frac{p^{2a+2b}}{p - p_1} = p^{a+2b} + p^{2a+2b-1} (1 + o(1)) \\ &= p^{a+2b} (1 + o(1)) \end{aligned}$$

where the last equality is from $a < 1$. Therefore, from (44) and (45), we obtain

$$\|\widehat{\mu}_D^*\|_2^2 = O_p(p^{a+2b}). \quad (51)$$

leading to

$$V = \frac{\widehat{\mu}_D^{*T} \mu_D^*}{\|\widehat{\mu}_D^*\|_2} \geq \frac{p^{a+2b} \{1 + o_p(1)\}}{O_p\{p^{(a+2b)/2}\}} \xrightarrow{P} \infty$$

for all $a, b > 0$.

B Lemmas for Theorem 1

We present the following three lemmas which are used in the proof of Theorem 1.

Lemma 1. For $p > 1$,

$$\left(1 - \frac{1}{p^2}\right)^p \geq 1 - \frac{1}{p}. \quad (52)$$

Proof. One can easily show that $f(x) = x \log\left(\frac{x+1}{x}\right)$ is an increasing function, by checking

$$f'(x) = \log\left(\frac{x+1}{x}\right) - \frac{1}{x+1}, \quad f''(x) = -\frac{1}{x(x+1)^2} < 0$$

and $\lim_{x \rightarrow \infty} f'(x) = 0$. From $f(p) \geq f(p-1)$, one can obtain

$$p \log\left(1 - \frac{1}{p^2}\right) \geq \log\left(1 - \frac{1}{p}\right),$$

which concludes the proof. \square

Lemma 2. Let $S_1, \dots, S_p \stackrel{\text{iid}}{\sim} N(0, 1)$ and $\Delta = p^b$. For $b < 0$ and the constant $a_n = (1/n_1 + 1/n_2)^{-1/2}$,

$$P\left(\max_{1 \leq j \leq p} |S_j| + a_n \Delta < \log p\right) > 1 - \frac{1}{p} \quad (53)$$

holds for large enough p .

Proof. Noting that for all $t > 0$, we have

$$\frac{t}{t^2 + 1} \phi(t) < 1 - \Phi(t) \leq \frac{1}{t} \phi(t)$$

where ϕ, Φ denote the probability distribution function and the cumulative distribution function of standard normal distribution, we obtain

$$P \left(\max_{1 \leq j \leq p} |S_j| + a_n \Delta < \log p \right) = \{1 - 2\Phi(a_n \Delta - \log p)\}^p \geq \left\{ 1 - \frac{2\phi(\log p - a_n \Delta)}{\log p - a_n \Delta} \right\}^p. \quad (54)$$

Since $a_n \Delta \rightarrow 0$ and $\log p \rightarrow \infty$ as $p \rightarrow \infty$, we have $2a_n \Delta < \log p$ for large p , therefore (54) satisfies the followings:

$$\begin{aligned} \left\{ 1 - \frac{2\phi(\log p - a_n \Delta)}{\log p - a_n \Delta} \right\}^p &\geq \left[1 - \frac{4\phi\{(\log p)/2\}}{\log p} \right]^p \\ &= \left[1 - \frac{4}{\sqrt{2\pi} \log p} \exp\{-(\log p)^2/8\} \right]^p. \end{aligned}$$

From lemma 1, for large p satisfying

$$\frac{4}{\sqrt{2\pi} \log p} \exp\left\{-\frac{(\log p)^2}{8}\right\} \leq \frac{1}{p^2},$$

we obtain

$$P \left(\max_{1 \leq j \leq p} |S_j| + a_n \Delta < \log p \right) \geq \left(1 - \frac{1}{p^2} \right)^p \geq 1 - \frac{1}{p}.$$

□

Lemma 3. Let $S_i \sim N(0, 1)$ and $\Delta = p^b$. Then, for $b < 0$ and $a_n = (1/n_1 + 1/n_2)^{-1/2}$, we

have

$$P\left(|S_i| + a_n\Delta < \sqrt{2\alpha(\log p + 1)}\right) > 1 - \frac{8}{\sqrt{2\alpha \log p}} \frac{e}{\sqrt{2\pi p^\alpha}} \quad (55)$$

for large enough p .

Proof. From the fact

$$\frac{t}{t^2 + 1}\phi(t) < 1 - \Phi(t) \leq \frac{1}{t}\phi(t),$$

for large enough p which satisfy $a_n\sqrt{2\alpha(\log p + 1)} < p^{-b} = 1/\Delta$ and $\sqrt{2\alpha(\log p + 1)} - 1 > \sqrt{2\alpha \log p} / 2$, we obtain

$$\begin{aligned} & P\left(|S_i| + a_n\Delta < \sqrt{2\alpha(\log p + 1)}\right) \\ &= 1 - 2\Phi\left(\sqrt{2\alpha(\log p + 1)} - a_n\Delta\right) \\ &> 1 - \frac{2}{\sqrt{2\pi}} \frac{2}{\sqrt{2\alpha(\log p + 1)} - a_n\Delta} \exp\left\{-\frac{1}{2}(\sqrt{2\alpha(\log p + 1)} - a_n\Delta)^2\right\} \\ &> 1 - \frac{4}{\sqrt{2\alpha(\log p + 1)} - 1} \frac{1}{\sqrt{2\pi p^\alpha}} \exp\left\{a_n\Delta\sqrt{2\alpha(\log p + 1)}\right\} \\ &> 1 - \frac{8}{\sqrt{2\alpha \log p}} \frac{e}{\sqrt{2\pi p^\alpha}}. \end{aligned}$$

□

Lemma 4. For $\widehat{\mu}_{D,i}^{EB}$ defined in (23), we have the lower bound W_i such that

$$\sum_{i=1}^{p_1} \widehat{\mu}_{D,i}^{EB} \geq \sum_{i=1}^{p_1} W_i \geq \frac{h^2}{1+h^2} a_n p^{a+b} \{1 + o(1)\} + o_p\{(\log p)^2\}$$

where

$$W_i = \begin{cases} W_{1i}, & \text{if } |S_i| + a_n\Delta \leq \sqrt{2\alpha(\log p + 1)} \\ W_{2i}, & \text{o.w} \end{cases}, \quad (56)$$

and

$$W_{1i} = \frac{h^2 S_i^*}{1+h^2} - \frac{h^2}{1+h^2} \frac{(1+2\sqrt{2\pi}p^{1/2+\epsilon})\sqrt{2\alpha(\log p+1)} + (1+h^2)/h^4}{p^{1-\alpha}(1-p^{a-1}) - 2p^{1/2+\epsilon}},$$

$$W_{2i} = \Delta + \frac{1}{a_n}(1-\log p)S_i - \frac{1}{a_n h^2} \log p.$$

Proof. • First, we consider Z_i as the following one :

$$Z_i = \begin{cases} Z_{1i}, & \text{if } |S_i| + a_n \Delta \leq \sqrt{2\alpha(\log p+1)} \\ Z_{2i}, & \text{o.w} \end{cases} \quad (57)$$

where

$$Z_{1i} = \Delta + \frac{S_i}{a_n} - \frac{1}{h^2} \frac{\frac{1}{\sqrt{2\pi}} \frac{h^3}{(1+h^2)^{3/2}} \{(p_1-1)S_i T_i + (p-p_1)S_i^* T_i^*\} + 2p^{1/2+\epsilon}}{\frac{1}{\sqrt{2\pi}} + \frac{1}{\sqrt{2\pi}} \frac{h}{(1+h^2)^{1/2}} \{(p_1-1)T_i + (p-p_1)T_i^*\} - 2p^{1/2+\epsilon}},$$

$$Z_{2i} = \Delta + \frac{S_i}{a_n} + \frac{1}{a_n h^2} \min \{(S_{ji}^-)_{1 \leq j \leq p_1}, (S_{ji}^- + a_n \Delta)_{p_1+1 \leq j \leq p}\}.$$

We first notice that Z_{1i} is constructed so that we have $\widehat{\mu}_{D,i}^{EB} \geq Z_{1i}$ on $E = \cap_{i=1}^{p_1} E_i$.

We also have $\widehat{\mu}_{D,i}^{EB} \geq Z_{2i}$ from (27).

• In addition, one can rewrite Z_{1i} as

$$Z_{1i} = \frac{h^2 S_i^*}{1+h^2} + \frac{\frac{1}{\sqrt{2\pi}} \left(\frac{h^2 S_i^*}{1+h^2} + \frac{h(p_1-1)a_n \Delta T_i}{(1+h^2)^{3/2}} \right) - 2p^{1/2+\epsilon} \left(\frac{h^2 S_i^*}{1+h^2} + \frac{1}{h^2} \right)}{\frac{1}{\sqrt{2\pi}} + \frac{1}{\sqrt{2\pi}} \frac{h \{(p_1-1)T_i + (p-p_1)T_i^*\}}{(1+h^2)^{1/2}} - 2p^{1/2+\epsilon}}$$

where S_i^* is defined in (21).

By plugging in the inequality $|S_i| + a_n\Delta \leq \sqrt{2\alpha(\log p + 1)}$ in Z_{1i} and the condition from E_{5i} for Z_{2i} , we obtain $W_i \leq Z_i$ on the event E when W_i is defined as follows:

By defining W_i , we obtained the the lower bounds of $\widehat{\mu}_{D,i}^{EB}$ which are mutually independent. Therefore, by applying the Weak Law of Large Numbers (WLLN) for triangular arrays on W_i , we can conclude the proof using (42).

For large enough p which satisfies

$$\log p \geq \sqrt{2\alpha(\log p + 1)}, \quad (58)$$

$$|W_{1i}| \leq \frac{h^2}{1+h^2} \left\{ \log p + \frac{(1 + 2\sqrt{2\pi}p^{1/2+\epsilon}) \log p + (1+h^2)/h^4}{p^{1-\alpha}(1-p^{a-1}) - 2p^{1/2+\epsilon}} \right\}$$

and

$$|W_{2i}| \leq \Delta + 2(\log p)^2/a_n$$

holds on E since $\max_{1 \leq i \leq n} |S_i| < \log p$ and $1/h^2 = \log p$. Therefore,

$$|W_i| \leq 1 + 2(\log p)^2/a_n.$$

In addition, for large enough p satisfying (58), one can obtain

$$\begin{aligned} E[W_1] &= E \left[W_{1i} \mid |S_i| + a_n\Delta \leq \sqrt{2\alpha(\log p + 1)} \right] \times P \left(|S_i| + a_n\Delta \leq \sqrt{2\alpha(\log p + 1)} \right) \\ &\quad + E \left[W_{2i} \mid |S_i| + a_n\Delta > \sqrt{2\alpha(\log p + 1)} \right] \times P \left(|S_i| + a_n\Delta > \sqrt{2\alpha(\log p + 1)} \right) \\ &> \left\{ \frac{h^2}{1+h^2} a_n\Delta - \frac{1 + 2\sqrt{2\pi}p^{1/2+\epsilon} + \log p}{p^{1-\alpha}(1-p^{a-1}) - 2p^{1/2+\epsilon}} \right\} (1-\gamma) + \left(\Delta - \frac{1}{a_n h^2} \log p \right) \gamma, \end{aligned}$$

where we define $\gamma = P\left(|S_i| + a_n\Delta > \sqrt{2\alpha(\log p + 1)}\right)$. Note that

$$E\left[S_i \mid |S_i| < c\right] = 0.$$

By applying lemma 3 and comparing the order of p in each term, one can obtain that for b which satisfy $b > \alpha + \epsilon - 1/2$ and $b > -\alpha$,

$$E[W_1] \geq \frac{h^2}{1+h^2} a_n \Delta \{1 + o(1)\}$$

holds. Note that when $b > -1/4$, in which all $(a, b) \in \mathcal{R}_{NPEB}$ with $b < 0$ are included, we can always pick such $\alpha, \epsilon > 0$ as $\epsilon = b + 1/4$, $\alpha = 1/4$. From the WLLN for triangular arrays,

$$\frac{\sum_{i=1}^{p_1} W_i - p_1 E[W_1]}{1 + 2(\log p)^2/a_n} \xrightarrow{p} 0. \quad (59)$$

Therefore, one can write

$$\sum_{i=1}^{p_1} W_i \geq \frac{h^2}{1+h^2} a_n p^{a+b} \{1 + o(1)\} + o_p\{(\log p)^2\}.$$

□